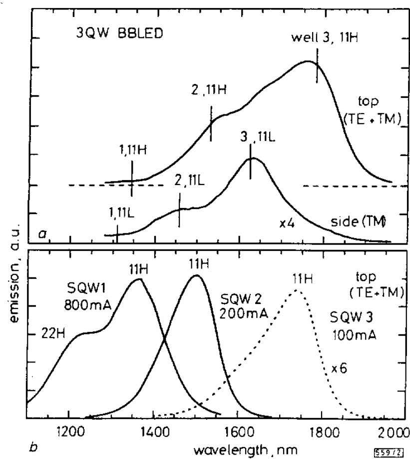

Fig. 2 *Emission spectra from triple quantum well LED and three single quantum well LEDs having wells similar to those in the triple-well structure*

a Triple quantum well LED
b Three single quantum well LEDs

(with TM-mode polarisation). In the TM spectrum, heavy-hole transitions are forbidden to first order, and we expect the $n = 1$ light-hole transitions (11L) to dominate. For top emission, both heavy-hole and light-hole transitions are allowed, but the $n = 1$ heavy-hole transitions (11H) are expected to dominate, because of the large heavy-light hole splittings due to the compressive strains. We have predicted the positions of the 11H and 11L transitions in our structures by using a tunnelling resonance calculation in the two-band envelope-function formalism. The results are shown as vertical bars in Fig. 2*a*. The predicted line positions agree well with measured features in the spectra, although the emission from well 1 (near 1.3μm) is quite weak. Note that this device has useful output between 1.40 and 1.90μm, a range of 500nm.

The relatively weak output of well 1 is confirmed in Fig. 2*b*, where we see that SQW1 requires about four times as much drive current as SQW2 for the same peak output. In addition, much of the emission from SQW1 is from the $n = 2$ heavy-hole transition (HH2) Thus it appears that the emission from well 1 in the triple-well structure is weak due to it being inefficient both in capturing carriers and in thermalising those that it does capture down to the ground state. Studies of carrier capture in quantum wells have shown that the capture and radiation processes depend strongly on the details of the energy level structure of the system [3]. To improve the emission of wells 1 and 2 in our structure, we have grown a structure where their widths are increased to 13 and 11.5nm, respectively. Calculations show that each well should now confine three electron levels, with the $n = 3$ levels all being near the tops of the wells. In contrast, the structure with 10nm thick wells only confines two levels in wells 1 and 2. In Fig. 3, we show the top emission from our second triple quantum well structure at three current levels. The emissions from wells 1 and 2 have been significantly enhanced relative to well 3, with the second well actually having the strongest output. Further work to improve the balance of the three emission lines is in progress.

Measured angular dependences of top emission at several wavelengths show an approximately cosinusoidal dependence. From this dependence we estimate an integrated top emission intensity of approximately 250μW. Measurements of current-voltage characteristics on devices of different areas, along with visual observations using an infrared viewer, show that our devices suffer from current crowding effects at operational currents. Preliminary data on edge emission from fully electroded bars suggest that integrated single-surface outputs of 1mW can easily be achieved with our structures.

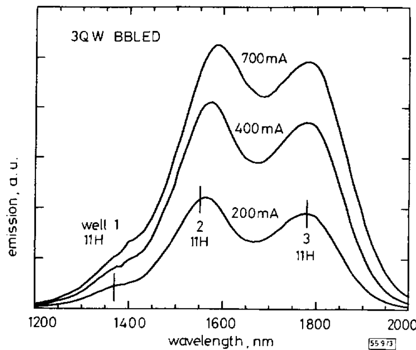

Fig. 3 *Top-emission spectra of a triple quantum well structure with well widths modified to improve carrier capture and radiation*

In conclusion, we have demonstrated a method of incorporating compressively strained quantum wells with a range of bandgaps into a broadband LED structure. Significant emission has been obtained over a wavelength range of ~500nm in the near infrared. Our technique should be applicable to other near-infrared wavelength ranges for a variety of sensing and spectroscopic applications.

Acknowledgments: It is a pleasure to acknowledge expert technical assistance from J.L. Dishman, J. Avery and J.M. Sergeant. This work was supported by the United States Department of Energy under Contract DE-AC04-94AL85000.

© IEE 1995
13 March 1995
Electronics Letters Online No: 19950555

I.J. Fritz, J.F. Klem, M.J. Hafich and A.J. Howard (*Sandia National Laboratories, Albuquerque, New Mexico 87185-0603, USA*)

References

1 MOSELEY, A.J., ROBBINS, D.J., MEATON, C., ASH, R.M., NICKLIN, R., BROMLEY, P., BRADLEY, R.R., CARTER, A.C., HONG, C.S., and FIGUEROA, L.: 'Broadband GaAs/Al$_x$Ga$_{1-x}$ multi-quantum well LED', Quantum Optoelectronics 1991, Technical digest series, (Optical Society of America, Washington, 1991), **7**, pp. 193–196

2 WANG, X., VAUGHAN, D.E., PELEKHATY, V., and CRISP, J.: 'A novel miniature spectrometer using an integrated acousto-optic tunable filter', *Rev. Sci. Instrum.*, 1994, **65**, pp. 3653–3656

3 BRUM, J.A., and BASTARD, G.: 'Resonant carrier capture by semiconductor quantum wells', *Phys. Rev. Lett.*, 1986, **33**, pp. 1420–1423

GaInAsSb/GaSb infrared photodetectors prepared by MOCVD

B. Zhang, T. Zhou, H. Jiang, Y. Ning and Y. Jin

Indexing terms: Chemical vapour deposition, infrared detectors

GaInAsSb/GaSb heterojunction photodetectors have been grown by metalorganic chemical vapour deposition (MOCVD). The room temperature performances of the photodetectors are described. The responsivity spectrum is peaked at 2.25μm and cut off at 1.7μm in the short wavelength and at 2.4μm in the long wavelength, respectively. The room temperature detectivity D^* is 10^9cm Hz$^{1/2}$ W^{-1} at 2.25μm.

$Ga_xIn_{1-x}As_{1-y}Sb_y$/GaSb quaternary alloys lattice-matched to GaSb are attractive materials for use in detectors and emitters in the 1.7 – 4.4μm infrared region. It has been suggested that GaIn-

AsSb infrared devices might have an advantage of operating at higher temperature or at room temperature. This virtue of GaInAsSb infrared devices meets the requirement of practical optoelectronic systems applied in outdoor environments and the military. Room temperature operation at wavelengths from 2.2 to 2.3μm has been reported for GaInAsSb/AlGaAsSb double heterostructure lasers grown by liquid phase epitaxy [1] and by molecular beam epitaxy [2]. In addition, GaInAsSb/GaSb photodiodes operating over the 1.8 – 2.3μm wavelength region have been reported [3].

In this Letter, we present the room temperature performances of back-illuminated *p*-GaInAsSb/*n*-GaSb heterojunction detectors operating over the 1.7 – 2.4μm wavelength region.

The *p*-GaInAsSb/*n*-GaSb heterojunctions were grown by metalorganic chemical vapour deposition at atmospheric pressure using trimethylgallium (TMGa), trimethylindium (TMIn), trimethylantimony (TMSb) and 10% arsine (AsH_3) diluted in hydrogen as the source materials. Palladium-diffused pure hydrogen was used as the carrier gas in the epitaxial growth. The GaSb substrates were etched by a mixed solution of acetic acid, hydrochloric acid and nitric acid (CH_3COOH:HCl:HNO_3 = 50:10:1).

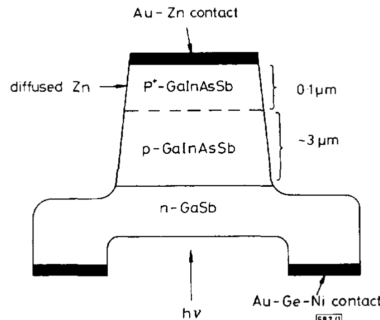

Fig. 1 *Schematic cross-section of back-illuminated GaInAsSb/GaSb photodetector*

Fig. 1 shows the schematic cross-section of the GaInAsSb/GaSb photodetector structure. The structure consists of three layers. The *n*-type (Te doped) GaSb substrate, with orientation 2° off (100) towards (110), has a net donor concentration of $5 \times 10^{17} cm^{-3}$. The undoped *p*-type $Ga_xIn_{1-x}As_{1-y}Sb_y$ epitaxial layer, with composition $x = 0.80$, $y = 0.82$, has a room temperature bandgap of 0.534eV, corresponding to a wavelength of 2.32μm. The epitaxial layer thickness is ~3μm. To form a highly conductive contact layer, a thin top layer of p^+-GaInAsSb ($10^{18} cm^{-3}$) was processed with Zn diffusion to a depth of the GaInAsSb epitaxial layer of ~0.1μm. The ohmic contacts were evaporated and alloyed, Au-Zn to the p^+-GaInAsSb layer and Au-Ge-Ni to the *n*-GaSb substrate, respectively.

The mesa geometry of the detector was defined using standard photolithographic techniques, and formed using a potassium iodide/iodine etching solution. The mesa diameter was 100μm, which resulted in an active area of $7 \times 10^{-5} cm^2$. A hole opened in the *n*-side metallisation and etched partly through the *n*-GaSb substrate permitted back-illumination of the photodetector. The back-illuminated configuration, as reported in [4], can minimise the active area and provide improved photoresponse at the shorter wavelengths.

The undoped GaInAsSb epitaxial layer grown on a semi-insulating GaAs substrate with the same growth conditions as that grown on an *n*-GaSb substrate, has a low net acceptor concentration of $10^{16} cm^{-3}$, measured by the standard van der Paul method. This lower carrier concentration can provide the photodetector with a large depletion region. By contrast, doping compensation for obtaining a low carrier concentration usually results in the increase of ionised impurity scattering, and consequently leads to degradation of detector detectivity.

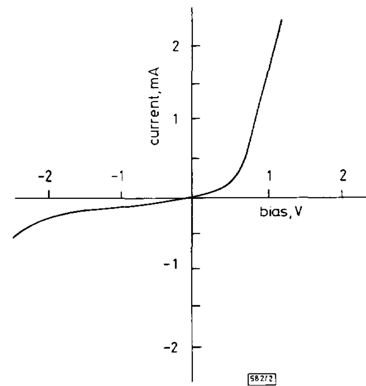

Fig. 2 *Dependence of dark current on voltage for p-GaInAsSb/n-GaSb photodetector*

Dark current against voltage at room temperature is shown in Fig. 2. The typical dark current is 50 – 100μA at –1V bias. It increases continuously with reverse bias without a break point. As a result, no definite breakdown voltage can be assigned. These results are similar to those reported by Srivastava *et al.* [3].

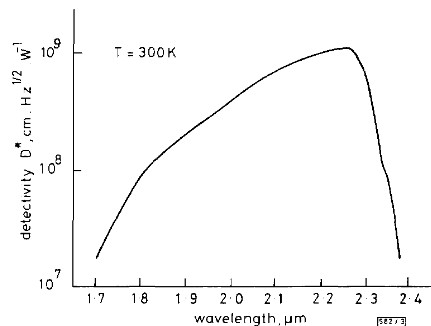

Fig. 3 *Responsivity spectrum for p-GaInAsSb/n-GaSb photodetector at zero bias*

The responsivity curve of the *p*-GaInAsSb/*n*-GaSb photodetector was measured with a 500K blackbody source and a single grating monochromator. Fig. 3 shows the responsivity spectrum at room temperature and zero bias. The spectrum is peaked at 2.25μm and cut off at the short wavelength of 1.7μm caused by absorption in the GaSb substrate, and cut off at the long wavelength of 2.4μm caused by the absorption edge of the GaInAsSb layer. At the peak wavelength of 2.25μm, the room temperature detectivity D^* is $10^9 cm\ Hz^{1/2}\ W^{-1}$ and the external quantum efficiency is ~30% with zero bias.

Conclusion: We have grown *p*-GaInAsSb/*n*-GaSb heterojunction structure for infrared photodetector fabrication via MOCVD and described the room temperature performances of the photodetector, which exhibit the photoresponse maximum in the 1.7 – 2.4μm spectral region and the detectivity D^* at 2.25μm of $10^9 cm\ Hz^{1/2}\ W^{-1}$.

Acknowledgments: The authors are grateful to P. Huan for device processing, and to J. Yuan and H. Song for helpful discussion. Thanks are due to Nation Advanced Materials Committee of China for financial support.

© IEE 1995
15 March 1995
Electronics Letters Online No: 19950525

B. Zhang, T. Zhou, H. Jiang, Y. Ning and Y. Jin (*Changchun Institute of Physics, Chinese Academy of Sciences, Changchun 130021, People's Republic of China*)

References

1 ZYSKIND, J.L., DEWINTER, J.C., BURRUS, C.A., CENTANNI, J.C., DENTAI, A.G., and POLLACK, M.A.: 'Highly uniform, high quantum efficiency GaInAsSb/AlGaAsSb double heterostructure lasers emitting at 2.2μm', *Electron. Lett.*, 1989, **25**, (9), pp. 568–570

2 EGLASH, S.J., CHOI, H.K., and TURNER, G.W.: 'MBE growth of GaInAsSb/AlGaAsSb double heterostructure for infrared diode lasers', *J. Cryst. Growth*, 1991, **111**, (1–4), pp. 669–676

3 SRIVASTAVA, A.K., DEWINTER, J.C., CANEAU, C., POLLACK, M.A., and ZYSKIND, J.L.: 'High performance GaInAsSb/GaSb p-n photodiodes for the 1.8–2.3 μm wavelength range', *Appl. Phys. Lett.*, 1986, **48**, (14), pp. 903–904

4 LEE, T.P., BURRUS, C.A., OGAWA, K., and DENTAI, A.G.: 'Very-high-speed back-illuminated InGaAs/InP pin punch-through photodiodes', *Electron. Lett.*, 1981, **17**, (12), pp. 431–432

Integrated quantum well intersub-band photodetector and light emitting diode

H.C. Liu, J. Li, Z.R. Wasilewski and M. Buchanan

Indexing terms: Integrated optoelectronics, Infra-red detectors, Infra-red imaging, Light emitting diodes

The authors propose and demonstrate the integration of a quantum well intersub-band photodetector (QWIP) and a light emitting diode (LED) for making large two-dimensional focal plane arrays for thermal imaging applications. The newly developed QWIP technology is combined with the well established LED technology both based on GaAs and related epitaxially grown alloys, such as AlGaAs and InGaAs.

The proposed device described here is intended for thermal imaging applications using large two-dimensional focal plane arrays (FPAs) in the mid and far infra-red (M&FIR) region of wavelength longer than 2μm. The conventional approach uses an InSb or an HgCdTe detector array hybrid bonded to an Si chip for multiplexing. We propose and demonstrate an integrated device comprising a quantum well intersub-band photodetector (QWIP) and a light emitting diode (LED). We combine the newly developed QWIP technology [1] with the well-established LED technology both based on GaAs and related epitaxially grown alloys, such as AlGaAs and InGaAs. The advantage of this unique approach over the conventional approach is that it uses a mature materials system and avoids hybrid bonding and any thermal mismatch.

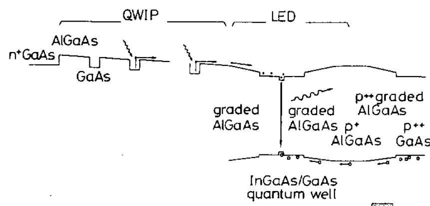

Fig. 1 *Band-edge profile of proposed integrated quantum well intersub-band photodetector (QWIP) and light emitting diode (LED)*

For the QWIP part, only the conduction band edge is shown

The basic idea is to integrate a QWIP with an LED by epitaxially growing them on top of each other. The QWIP can be either *n*-type or *p*-type. Fig. 1 shows a GaAs/AlGaAs *n*-QWIP with an InGaAs/GaAs quantum well LED. Only two contacts are made: one to the heavily *p*-doped LED contact layer and one to the heavily *n*-doped QWIP emitter. A forward bias is applied to this serial QWIP-LED, which should be large enough to turn both the QWIP and the LED to their operating bias conditions. For concreteness, we assume that the QWIP detects M&FIR light of wavelength greater than 2μm and that the LED emits in the near-infra-red (NIR) region of wavelength 800 – 1000nm. The QWIP is a photoconductor so that under M&FIR light illumination its resistance changes, which leads to a change in the amount of NIR emission. This device is therefore an M&FIR to NIR converter. For 77K operation, a well designed QWIP can be very efficient [2] with 20% absorption easily achieved when the LED technology is well developed. An optimised QWIP-LED can therefore be very efficient with very little or no loss of performance compared to when the QWIP alone is used as an M&FIR detector. However, the advantage of this integrated QWIP-LED is of extreme importance technologically. In this scheme, large format two-dimensional FPAs can be made with a high pixel fill factor without the need to integrate any circuits on the FPA chip and without the need for hybrid bonding with another multiplexer chip (normally Si). This also avoids the thermal mismatch problem which occurs in large format hybrid FPAs at the cryogenic temperatures which are required for high performance M&FIR detectors. The resulting NIR emission can be easily imaged using another well developed device: an Si-CCD which has a spectral response matched to the NIR wavelength.

To demonstrate the basic concept, we have grown a test structure using a molecular beam expitaxy system. Starting with a semi-insulating (100) GaAs substrate, a QWIP structure for a peak detection wavelength of 9μm in the FIR was grown, followed by an InGaAs/GaAs quantum well LED. The QWIP consisted of the following layers (in growth sequence): a bottom contact layer of 800nm n^+-GaAs doped with Si to a density of $1.5 \times 10^{18} cm^{-3}$, a 5nm GaAs spacer, and 50 more $Al_{0.25}Ga_{0.75}As$/GaAs quantum wells with a 40nm barrier and 5.9nm well. The wells were doped with an Si-δ-spike to a density of $5 \times 10^{11} cm^{-2}$. These δ-spikes were positioned away from the well centre towards the substrate by ~2.5nm to counterbalance the Si segregation during growth and ensure the symmetry of the QWIP structure [3]. Growth continued with the following LED layers: a 40nm graded $Al_xGa_{1-x}As$ layer from $x = 0.25$ to 0.12, a 30nm GaAs, a 7.0nm $In_{0.2}Ga_{0.8}As$ well, a 30nm GaAs, a 40nm graded $Al_xGa_{1-x}As$ layer from $x = 0.12$ to 0.25, a 50nm $p^+Al_{0.25}Ga_{0.75}As$ with Be doping graded from 1 to $8 \times 10^{18} cm^{-3}$, a 40nm graded $p^{++}Al_xGa_{1-x}As$ layer from $x = 0.25$ to 0.12 with its doping increased from 8×10^{18} to $10^{19} cm^{-3}$, and finally a 200nm p^{++}GaAs top contact layer with $10^{19} cm^{-3}$ doping. The advantage of using InGaAs as the well material is that the emitted light is not absorbed in any other layers.

Mesa devices with area of $290 \times 140 \mu m^2$ were made using standard GaAs lithography techniques. The top *p*-type contacts were narrow ring shaped near the mesa edge resulting in an emission window of $200 \times 100 \mu m^2$ for the NIR light from the LED. A 45° edge facet was polished near the devices to facilitate FIR coupling to the intersub-band transition [4]. The device was mounted in a 77K cold-finger optical cryostat, and actual device temperature was estimated to be 82K. A 1000K blackbody source or a CO_2 laser was used as the FIR source. A grating monochromator or a Fourier transform spectrometer was used for wavelength selection. An Si photodiode was used to measure the NIR emission.

Fig. 2 summarises the experimental results. Since the QWIP and the LED are in series, the bias current is common. Fig. 2*a* shows the LED emitted power at a wavelength of 927nm against bias current. The inset shows schematically the device geometry. Fig. 2*b* presents the QWIP responsivity for unpolarised light at a wavelength of 9.2μm. The insets are the schematic device geometry and the normalised spectral response. Fig. 2*c* gives the measured increase of the LED emission for several FIR power values at a wavelength of 9.2μm.

Given our simple LED device structure, the observed external efficiency is only ~0.8% as calculated from Fig. 2*a* by comparing the output photon rate (photon/s) with the input current (electron/s). Assuming a near unity internal efficiency, which is realistic for our high quality InGaAs/GaAs quantum wells, two main factors lead to the low external efficiency. First, the top ring contact metal blocks part of the emission. The ratio of the emit-